

Large eddy simulations of round free jets using explicit filtering with/without dynamic Smagorinsky model

Christophe Bogey*, Christophe Bailly

Laboratoire de Mécanique des Fluides et d'Acoustique, UMR CNRS 5509, Ecole Centrale de Lyon, 69134 Ecully Cedex, France

Available online 23 March 2006

Abstract

Large eddy simulations (LES) of round free jets at Mach number $M=0.9$ with Reynolds numbers over the range $2.5 \times 10^3 \leq Re_D \leq 4 \times 10^5$ are performed using explicit selective/high-order filtering with or without dynamic Smagorinsky model (DSM). Features of the flows and of the turbulent kinetic energy budgets in the turbulent jets are reported. The contributions of molecular viscosity, filtering and DSM to energy dissipation are also presented. Using filtering alone, the results are independent of the filtering strength, and the effects of the Reynolds number on jet development are successfully calculated. Using DSM, the effective jet Reynolds number is found to be artificially decreased by the eddy viscosity. The results are also not appreciably modified when subgrid-scale kinetic energy is used. Moreover, unlike filtering which does not significantly affect the larger computed scales, the eddy viscosity is shown to dissipate energy through all the turbulent scales, in the same way as molecular viscosity at lower Reynolds numbers.

© 2006 Elsevier Inc. All rights reserved.

Keywords: Large eddy simulation; Jet; High-order filtering; Subgrid model

1. Introduction

In simulations, important issues need to be addressed to ensure that the solutions are physically correct and that they are not artifacts of the computational procedure. This is particularly the case for the numerical dissipation, whose effects are to be minimized so that they do not exceed the physical mechanisms. In large eddy simulation (LES) where only the turbulent scales discretized by the grid are calculated, this point is particularly crucial. The scales affected by viscous diffusion are indeed lacking. An artificial damping is therefore required to dissipate the turbulent kinetic energy, and in practice to enforce stability.

An eddy viscosity is generally introduced in LES to account for the dissipative effects of the subgrid scales. The widely-used dynamic Smagorinsky model (DSM) is based on this hypothesis. In this model, especially devel-

oped by Moin et al. (1991) for compressible turbulence, the eddy viscosity is expressed from physical considerations and its amplitude is estimated from the computed scales. However, the use of eddy viscosity in LES still raises important questions. For instance eddy-viscosity models might dissipate the turbulent energy excessively. They might also affect a wide range of turbulent scales up to the larger ones, even at high Reynolds numbers. Moreover, since eddy viscosity has the same functional form as molecular viscosity, it is difficult to define the effective Reynolds number of the simulated flows (Domaradski and Yee, 2000; Bogey and Bailly, 2005b).

Alternatives to the eddy-viscosity approach, based on filtering for modelling the effects of the subgrid scales, have been proposed. One way consists in using low-dissipative schemes for time and space discretization, while explicitly applying a compact/selective filter to the flow variables with the aim of affecting only the wave numbers located near the grid cutoff wave number. In this case, the dissipation on the larger resolved scales is minimized and energy is only removed when it is transferred to the smaller scales discretized by the mesh grid. This LES methodology was

* Corresponding author. Tel.: +33 4 72 18 60 18; fax: +33 4 72 18 91 43.
E-mail addresses: christophe.bogey@ec-lyon.fr (C. Bogey),
christophe.bailly@ec-lyon.fr (C. Bailly).
URL: <http://acoustique.ec-lyon.fr> (C. Bogey).

recently successfully applied to isotropic turbulence, channel flows and jets (Visbal and Rizzetta, 2002; Rizzetta et al., 2003; Mathew et al., 2003; Bogey and Bailly, 2006a). Visbal and Rizzetta (2002) obtained for instance better results using filtering alone than with Smagorinsky models for isotropic turbulence. In their approximate deconvolution model, Stolz et al. (2001) also introduced a relaxation term that is very similar to the explicit selective filtering. Their LES of channel flows showed a significant improvement over the results obtained using DSM.

The channel flow configuration is indeed one of the most considered test cases in numerical fluid dynamics. Simulations of free shear flows have however been developed over the last few years. Large eddy simulations have for instance been performed with the aim of investigating the noise generated by round jets, as illustrated by the recent papers of Andersson et al. (2005), Bodony and Lele (2005) and Bogey and Bailly (2006a,b). Free shear flows have also been computed in order to study subgrid modelling in LES. Subgrid models have thus been evaluated by comparing LES results to results obtained by direct numerical simulation (DNS) for mixing layers and plane jets (Vreman et al., 1997; Le Ribault et al., 1999). The grid/subgrid-scale interactions have moreover been analysed from DNS database of planar jets (Akhavan et al., 2000; Da Silva and Métais, 2002).

In the present study, Large eddy simulations of round free jets at Mach number $M = u_j/c_0 = 0.9$ (u_j is the jet exit velocity, c_0 the speed of sound in the ambient medium) are reported. The simulations are performed with low-dissipative numerical schemes (Bogey and Bailly, 2004), using explicit selective/high-order filtering with or without dynamic Smagorinsky model. A jet at a high Reynolds number $Re_D = u_j D/\nu = 4 \times 10^5$ (D is the jet diameter, ν the kinematic molecular viscosity) was first simulated by the authors (Bogey and Bailly, 2006a) using filtering alone. The computed flow and sound fields were found to be in agreement with measurements at high Reynolds numbers. This jet at $Re_D = u_j D/\nu = 4 \times 10^5$ is now simulated using a filtering of different strength. It is also computed using DSM involving eddy-viscosity with or without subgrid-scale kinetic energy. The motivation is here to study the influence of the filtering and of DSM on jet flow. Jets with lower Reynolds numbers over the range $2.5 \times 10^3 \leq Re_D \leq 10^4$ are also calculated using filtering alone, with the aim of reproducing the effects of the Reynolds number on jet development. These LES data at low Reynolds numbers will be compared to the DSM results at $Re_D = 4 \times 10^5$. Moreover, the dissipation mechanisms involved in the present LES, i.e., molecular viscosity, filtering and DSM, will be investigated. The dissipation rates due to these mechanisms will be evaluated from the energy budgets, and the affected scales will be characterized.

The present paper is organized as follows. First the parameters of the different simulations are described. Flow features obtained from the LES are then shown. The kinetic energy budgets are subsequently calculated, and the contributions of molecular viscosity, explicit filtering

Table 1

LES parameters: jet Reynolds numbers Re_D , frequencies of application of the filtering ($\Delta t = 0.85 \times (r_0/15)/c_0$ is the time step), dynamic Smagorinsky model (DSM) application and core lengths x_c

	Re_D	Filtering frequency	DSM	x_c/r_0
LESsf	4×10^5	$2\Delta t$	–	10.2
LESsf2	4×10^5	$3\Delta t$	–	10.2
LESdsm	4×10^5	$2\Delta t$	ν_t	10.4
LESdsm2	4×10^5	$2\Delta t$	$\nu_t + k_{sgs}$	10.4
LESre1	10^4	$2\Delta t$	–	10.7
LESre2	5×10^3	$2\Delta t$	–	11.3
LESre3	2.5×10^3	$2\Delta t$	–	13

and DSM to the dissipation are presented. Finally concluding remarks are drawn.

2. Simulations

The specifications of the simulations are given in Table 1. Initial conditions are defined for isothermal round jets with centerline velocities and diameters yielding a fixed Mach number $M = 0.9$ and various Reynolds numbers. LESsf, LESsf2, LESdsm and LESdsm2 jets are at the high Reynolds number of $Re_D = 4 \times 10^5$, while LESre1, LESre2 and LESre3 jets are at $Re_D = 10^4$, 5×10^3 and 2.5×10^3 , respectively.

The numerical algorithm is that of the reference simulation LESsf, described in detail and referred to as LESac in Bogey and Bailly (2006a). The filtered compressible Navier–Stokes equations are solved using numerical schemes developed in Bogey and Bailly (2004), which were optimized in the Fourier space in order to minimize the dispersion and the dissipation errors for the scales discretized by more than four grid points. Spatial derivatives are obtained by explicit fourth-order thirteen-point centered finite-differences. Time integration is taken in account by an explicit second-order six-stage Runge–Kutta algorithm. Grid-to-grid oscillations are removed by an explicit filtering, involving fourth-order thirteen-point and twenty-one-point filters, which were designed in order to damp the scales discretized by less than four grid points without affecting the larger scales. The filtering is applied explicitly to the density, momentum and pressure variables, every two or three iterations, sequentially in the grid directions. Note that, due to the explicit time integration, the time step is only $\Delta t = 0.85 \times (D/30)/c_0$. It is therefore expected to be quite smaller than the characteristic time scales of the turbulent flow. This is of importance in order to avoid an accumulation of energy at the smaller scales discretized. The computational domain is a 12.5 million point Cartesian grid with 15-points in the jet radius ($\Delta y = r_0/15$). The flow is computed axially up to $x = 25r_0$, and radially up to $y, z = 15r_0$. The discretizations in the y and z directions are indeed the same, and are symmetrical about the jet axis. The mesh spacing is moreover uniform in the jet flow with $\Delta y = \Delta z = \Delta x/2$. Finally, non-reflective bound-

ary conditions are used, with the addition of a sponge zone at the outflow.

In all simulations, mean axial velocity at the jet inflow boundary is defined by a hyperbolic-tangent profile with a ratio $\delta_0/r_0 = 0.05$ between the shear-layer momentum thickness and the jet radius. Mean radial and azimuthal velocities are set to zero, pressure is set to the ambient pressure, and the density profile is obtained from a Crocco–Busemann relation. To seed the turbulence, small random velocity disturbances are added in the shear layer following the procedure used in the LESsf simulation. The effects of the inflow conditions and forcing were investigated in Bogey and Bailly (2005a).

In LESsf and LESsf2, the selective filtering is used alone, every second and third iteration, respectively. In LESdsm and LESdsm2, filtering is applied as in LESsf but in combination with the dynamic Smagorinsky model (DSM). In the DSM, an eddy viscosity ν_t and a subgrid-scale kinetic energy k_{sgs} are introduced to approximate the deviatoric and isotropic parts of the subgrid stress tensor \mathcal{T}_{ij} , then expressed as

$$\mathcal{T}_{ij} = \bar{\rho} \tilde{u}_i \tilde{u}_j - \bar{\rho} \tilde{u}_i \tilde{u}_j \simeq 2\bar{\rho} \nu_t \tilde{S}_{ij}^D - (2/3)k_{sgs} \delta_{ij}$$

where the superscript *D* denote the deviatoric part, and the bar and tilde indicate the LES filterings for compressible turbulence, see Moin et al. (1991). The eddy viscosity is parameterized using the Smagorinsky model as $\nu_t = C\Delta^2\tilde{S}$, and the SGS kinetic energy as $k_{sgs} = \bar{\rho}C_1\Delta^2\tilde{S}^2$ where $\Delta = (\Delta x \Delta y \Delta z)^{1/3}$ and $\tilde{S} = (2\tilde{S}_{ij}\tilde{S}_{ij})^{1/2}$. The coefficients *C* and *C*₁ are computed using the dynamic procedure of Lilly (1992)

$$C = \langle L_{ij}^D M_{ij} \rangle / \langle M_{ij}^2 \rangle \quad \text{and} \quad C_1 = \langle L_{kk} \rangle / \langle N \rangle$$

where $\hat{\cdot}$ represents a 15-point stencil test filter of width $k_c \Delta x = \pi/2$ designed in Bogey and Bailly (2004), $\langle \cdot \rangle$ a second-order filter, and

$$\begin{cases} L_{ij} = \widehat{\rho u_i \rho u_j} / \widehat{\rho} - [\widehat{\rho u_i} \widehat{\rho u_j} / \widehat{\rho}]^{\wedge} \\ M_{ij} = 2\widehat{\rho} \widehat{\Delta}^2 \tilde{S} (\tilde{S}_{ij} - \tilde{S}_{kk} \delta_{ij} / 3) - [2\bar{\rho} \Delta^2 \tilde{S} (\tilde{S}_{ij} - \tilde{S}_{kk} \delta_{ij} / 3)]^{\wedge} \\ N = -2\widehat{\rho} \widehat{\Delta}^2 \tilde{S}^2 + [2\bar{\rho} \Delta^2 \tilde{S}^2]^{\wedge} \end{cases}$$

with $\tilde{\cdot}$ denoting test-filtered quantities. The SGS kinetic energy is used in the LESdsm2 simulation but $k_{sgs} = 0$ in LESdsm.

Profiles along the jet axis of the coefficients *C* and *C*₁ are presented in Fig. 1. The mean values of *C* in LESdsm and LESdsm2 are in particular very close. They are about 0.02 in the turbulent flow region, standing in the range of values obtained for isotropic turbulence from the Smagorinsky constant yielding $C_s^2 = 0.032$, or from numerical simulations (e.g., Speziale et al. (1988), Moin et al. (1991), Erlebacher et al. (1992)). The mean value of *C*₁ in LESdsm2 is about 0.01 and corresponds also fairly well to the values calculated for isotropic turbulence.

Axial profiles of the eddy viscosity and of the SGS kinetic energy are shown in Fig. 2. The simulations LES-

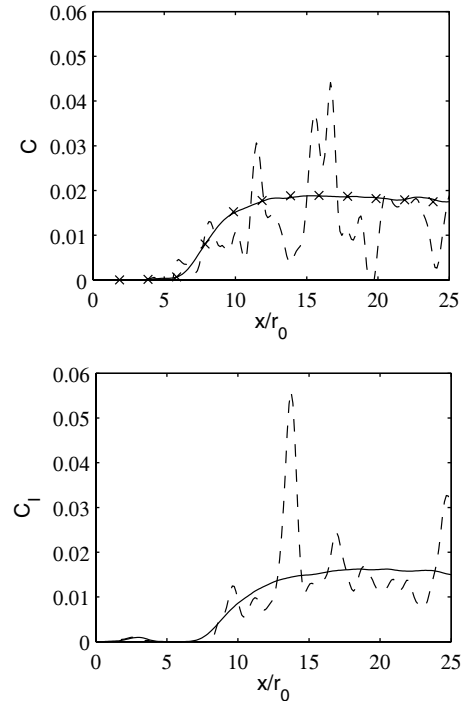


Fig. 1. Centerline profiles of the DSM coefficients *C* and *C*₁. Mean values: — LESdsm2, × LESdsm; instantaneous values: - - - LESdsm2.

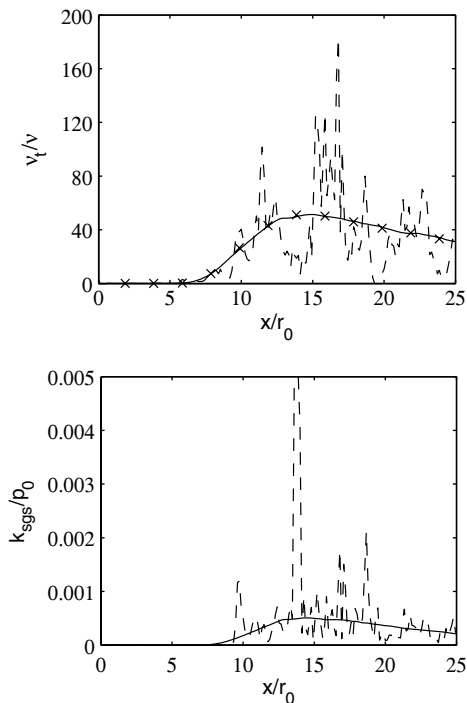


Fig. 2. Centerline profiles of the ratios ν_t/ν between eddy and molecular viscosities, and k_{sgs}/ρ_0 between SGS kinetic energy and ambient pressure. Mean values: — LESdsm2, × LESdsm; instantaneous values: - - - LESdsm2.

dsm and LESdsm2 provide mean values of eddy viscosity that are very similar. In the turbulent region, the eddy viscosity ν_t is of the order of fifty times the molecular

viscosity, which might lead to an effective Reynolds number of $\overline{Re}_D = u_j D / \nu_t \simeq 8 \times 10^3$, as already discussed in Bogey and Bailly (2005b). The SGS kinetic energy in LESdsm2 is found to be small with respect to the ambient pressure, with $k_{sgs}/p_0 \simeq 5 \times 10^{-4}$. This agrees with Erlebacher et al. (1992) who noticed that the isotropic part of the SGS tensor is dominated by the thermodynamic pressure in most turbulent flows.

Finally, in the simulations LESre1, LESre2 and LESre3, the filtering is used alone as in LESSf. Note that the two Reynolds numbers Re_D in LESre1 and LESre2 enclose the effective Reynolds number \overline{Re}_D expected using DSM in LESdsm.

3. Flow properties

Snapshots of vorticity are presented in Fig. 3 for the simulations LESSf and LESdsm at $Re_D = 4 \times 10^5$, and for LESre2 at the low Reynolds number of $Re_D = 5 \times 10^3$. The flow fields from LESSf and LESre2 show that the turbulent development of the jets depends appreciably on the Reynolds number. In LESSf at $Re_D = 4 \times 10^5$, the turbulent flow field displays a large range of vortical scales, whereas in LESre2 at $Re_D = 5 \times 10^3$ a part of the fine scale is lacking. Furthermore, as the Reynolds number decreases, the generation of vortical structures in the shear layer occurs farther downstream. This trend must be due to the decrease of the growth rates of instabilities by viscosity at low Reynolds numbers (Michalke, 1984). Consequently, the potential core length x_c , determined here from the centerline

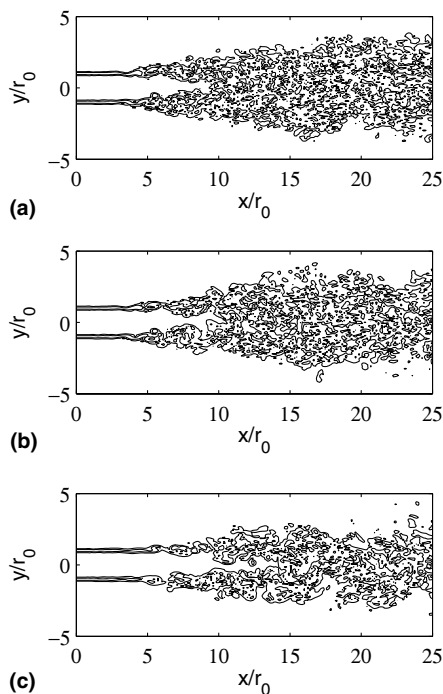


Fig. 3. Snapshots of vorticity in the plane $z=0$ for: (a) LESSf, (b) LESdsm, and (c) LESre2. Representation of the two vorticity-norm contours associated with the magnitudes $|\omega| \times r_0/u_j = [1.05, 3.15]$.

mean velocity u_c using $u_c(x_c) = 0.95u_j$, increases as the Reynolds number decreases, as reported in Table 1. The present core lengths are moreover comparable to the core lengths of $12r_0$ measured for Mach 0.9, transitional jets at both low and high Reynolds numbers by Stromberg et al. (1980) and Arakeri et al. (2003).

In LESdsm, the jet development appears fairly similar to that obtained in LESSf. The core lengths are for instance very close as shown in Table 1. This point must be related to the dynamic procedure which reduces the magnitude of the eddy viscosity in the transitional shear layer. However, there seems to be less fine scales in LESdsm than in LESSf, and the turbulent flow field from LESdsm appears intermediary between that from LESSf and that from LESre2.

The profiles of centerline mean axial velocity are presented in Fig. 4 for the different jets. They are shifted in the axial direction to yield identical core lengths x_c in order to compare properly the velocity decays after the potential core. The profiles from the LES at the high Reynolds number of $Re_D = 4 \times 10^5$ are plotted in Fig. 4(a). The velocity decay is clearly more rapid in the LES using DSM. Moreover the profiles from the simulations LESSf and LESSf2, where filtering is applied alone but at a different frequency, are identical. In the same way, using DSM with or without k_{sgs} in LESdsm and LESdsm2, the results do not differ appreciably.

The velocity profiles from LESSf, LESdsm and the LES at low Reynolds numbers are displayed in Fig. 4(b). The

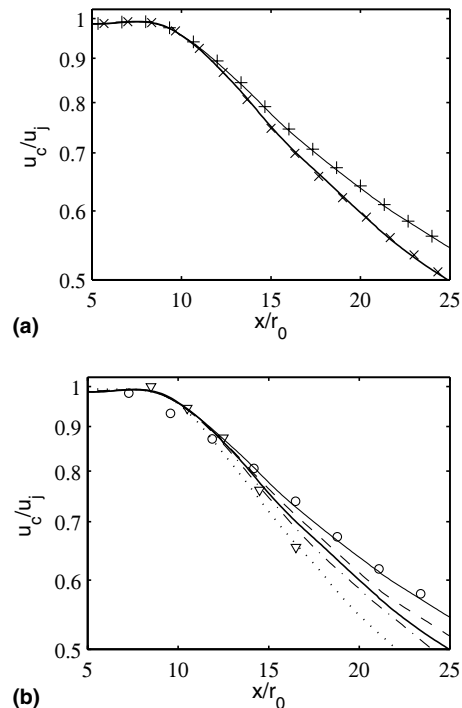


Fig. 4. Centerline mean axial velocity for: — LESSf, + LESSf2, — LESdsm, × LESdsm2, - - - LESre1, - · - · - LESre2, · · · · · LESre3. Measurements: ○ Arakeri et al. (2003) ($M=0.9$, $Re_D=5 \times 10^5$), ▽ Stromberg et al. (1980) ($M=0.9$, $Re_D=3.6 \times 10^3$). The profiles are shifted with respect to the LESSf profile to yield identical core lengths.

simulations LESsf, LESre1, LESre2 and LESre3, performed using filtering alone, provide velocity decays after the potential core that are faster as the Reynolds number decreases. This behaviour is in accordance with the experimental data available for $M = 0.9$ jets. The velocity decay of the LESre3 jet at $Re_D = 2500$ is indeed similar to that measured for a jet at $Re_D = 3600$ by Stromberg et al. (1980). A good agreement is also observed between the results from the high Reynolds number jet of LESsf and from the experimental, initially laminar jet at $Re_D = 5 \times 10^5$ of Arakeri et al. (2003). As for the velocity decay from LESdsm, it is found to stand between those from LESre1 and LESre2. This supports that using DSM the effective Reynolds number of the jet is reduced down to $\overline{Re}_D = u_j D / \nu_t \simeq 8 \times 10^3$.

The centerline profiles of the turbulent axial velocity u'_{rms} are now presented in Fig. 5. For the jets at $Re_D = 4 \times 10^5$, in Fig. 5(a), the peak of u'_{rms} is shown to be higher using DSM. In the same way as for the velocity decay in Fig. 4(a), there is also no significant effect of the filtering frequency nor of the subgrid-scale kinetic energy on the turbulence intensity.

In Fig. 5(b), the profiles from LESsf, LESre1, LESre2 and LESre3 indicate that the amplitude of the peak of u'_{rms} increases as the Reynolds number decreases. This trend is supported by direct numerical simulation (DNS) and measurements. The profile from the LESre3 jet at $Re_D = 2500$ compares indeed favorably with that from the DNS jet at $Re_D = 3600$ computed by Freund (2001), while the profile

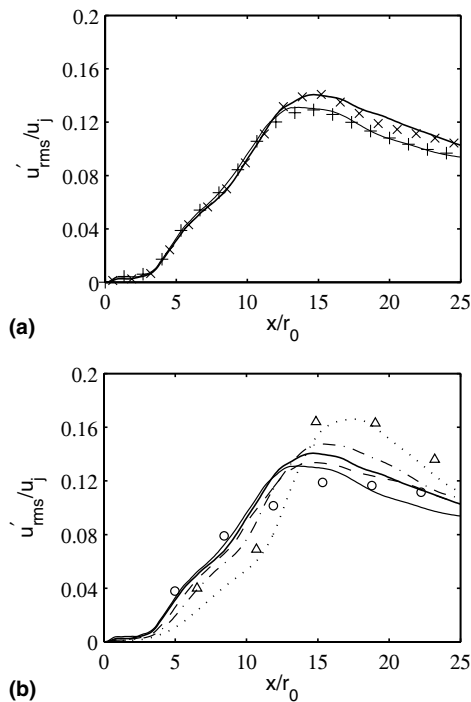


Fig. 5. Centerline profiles of the rms fluctuating axial velocity for: — LESsf, + LESsf2, — LESdsm, × LESdsm2, - - - LESre1, - · - · LESre2, · · · · · LESre3; ○ measurements of Arakeri et al. (2003) shifted axially by $-6.5r_0$ ($M = 0.9$, $Re_D = 5 \times 10^5$); △ DNS results of Freund (2001) shifted by $-1.8r_0$ ($M = 0.9$, $Re_D = 3600$).

from the LESsf jet at high Re_D agrees fairly well with that from the experimental jet at $Re_D = 5 \times 10^5$ of Arakeri et al. (2003). Finally note that the u'_{rms} peak from LESdsm is between those from LESre1 and LESre2.

4. Energy balance and dissipation mechanisms

The budget of the turbulent kinetic energy is now calculated in order to determine the contributions of the explicit filtering, molecular viscosity, and DSM to energy dissipation in the present LES. The filtering contribution is evaluated as the balance of all the other terms in the energy budget, calculated explicitly from the LES fields. The admissibility of doing so is justified by the negligible dissipation of the time-integration algorithm. The maximum amount of dissipation provided by the Runge–Kutta algorithm, obtained for the higher angular frequency resolved, is indeed only of 3×10^{-5} per iteration. Note that the higher angular frequency resolved, $(\omega \Delta t)_{max} = 1.63$, is deduced from the higher wave number calculated by the spatial scheme, $(k \Delta y)_{max} = 2.13$, for the present CFL number of 0.85 and a convection velocity of u_j . The equation for the energy budget is derived from the filtered Navier–Stokes equations given in Bogey and Bailly (2006a):

$$0 = \underbrace{-\frac{\partial}{\partial x_j} (k [u_j])}_{\text{advection}} - \underbrace{\langle \bar{\rho} u'_i u'_j \rangle \frac{\partial [u_i]}{\partial x_j}}_{\text{production}} - \underbrace{\frac{1}{2} \frac{\partial}{\partial x_i} \langle \bar{\rho} u_i'^2 u'_i \rangle}_{\text{turb.diffusion}} - \underbrace{\langle \bar{\tau}_{ij} \frac{\partial u'_i}{\partial x_j} \rangle}_{\text{visc.dissip}} - \underbrace{\langle \mathcal{T}_{ij} \frac{\partial u'_i}{\partial x_j} \rangle}_{\text{pressure diffusion}} + \frac{\partial}{\partial x_{ij}} \langle u'_i \bar{\tau}_{ij} \rangle + \frac{\partial}{\partial x_i} \langle u'_i \mathcal{T}_{ij} \rangle - \underbrace{\frac{\partial}{\partial x_i} \langle p' u'_i \rangle}_{\text{pressure diffusion}} + \langle p' \frac{\partial u'_i}{\partial x_i} \rangle - \langle u'_i \rangle \frac{\partial \langle p \rangle}{\partial x_i} + D_{\text{filter}}$$

where the turbulent kinetic energy is $k = \langle \bar{\rho} u_i'^2 / 2 \rangle$. Density, velocity and pressure are represented by ρ , u_i and p , the turbulent and subgrid stress tensors by τ_{ij} and \mathcal{T}_{ij} . The tilde and overbar indicate Favre and Reynolds grid-filtered quantities, and the prime fluctuating quantities. Statistical averaging is denoted by $\langle \cdot \rangle$, and $[u_i] = \langle \bar{\rho} u_i \rangle / \langle \bar{\rho} \rangle$. Except for the filtering dissipation D_{filter} , all the terms are calculated directly from the LES data. The main ones are those corresponding to meanflow advection, production, viscous dissipation, turbulence diffusion, pressure diffusion, and the possible DSM contribution. The present energy budget equation was recently used in Bogey and Bailly (2005c) for a jet at the same Reynolds number as that investigated experimentally by Panchapakesan and Lumley (1993). LES results and measurements were found in this case to agree very well.

As an illustration, the energy budget across $x = 20r_0$ is shown in Fig. 6 for the high Reynolds number simulation LESsf using filtering alone. We can notice that, the viscous dissipation being negligible, the dissipation is only due to the filtering. The present curves agree qualitatively fairly

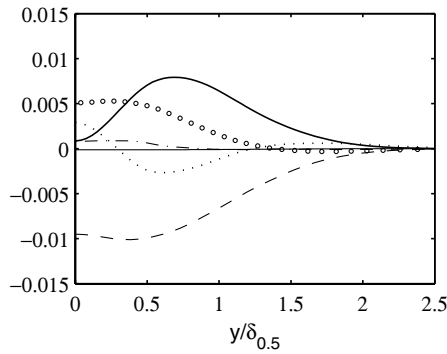


Fig. 6. Kinetic energy budget across $x = 20r_0$ for LESsf: $\circ\circ\circ\circ$ advection, — production, — viscous dissipation, - - - filtering dissipation, $\cdots\cdots$ turbulence diffusion, - · - · pressure diffusion. The curves are normalized by $\rho_c u_c^3 \delta_{0.5}$ (ρ_c and u_c centerline mean density and axial velocity, $\delta_{0.5}$: jet half-width).

well with corresponding experimental curves of the literature, see for instance Panchapakesan and Lumley (1993). However they must be compared with care because the location $x = 20r_0$ is far from the self-similarity region (Wynanski and Fiedler, 1969), where the measurements are done.

We now focus on the dissipation mechanisms involved in the LES, and more especially on their magnitudes evaluated from the energy budgets. Their contributions at $x = 20r_0$ are presented in Fig. 7 for LESsf and LESsf2, LESdsm2, and LESre2. The effects of molecular viscosity are found to be negligible in Fig. 7(a) and (b) for the jets at $Re_D = 4 \times 10^5$, but significant in Fig. 7(c) at $Re_D = 5 \times 10^3$. This results from the fact that, as the Reynolds number increases, the scales affected by molecular viscosity are smaller and tend to be not discretized by the grid. In particular at a sufficiently high Reynolds number, most of these scales are likely not to be resolved. In this case, the energy dissipation must be provided almost entirely by the SGS modelling.

In LESsf and LESsf2 using selective filtering alone, the energy dissipation is thus only supplied by the filtering as shown in Fig. 7(a). In these two LES, where the filtering is applied, respectively, every second and third iteration, the dissipation rates are moreover very close. This demonstrates that the dissipation rate in the present LES is independent of the filtering strength and, consequently, is determined only by physical mechanisms. This important feature is undoubtedly due to the high selectivity of the filtering which does not appreciably dissipate the scales discretized by more than four grid points. Energy is thus expected to be removed only when it is transferred from the large scales to the small scales affected by the filtering. In LESdsm2, the energy dissipation is also taken into account by the DSM. In Fig. 7(b), it thus appears to be ensured both by the filtering and by the eddy viscosity, in comparable proportions. We can finally note that the contribution of the SGS energy is negligible, as suggested by Erlebacher et al. (1992) and by the very small values of k_{sgs} displayed in Fig. 2.

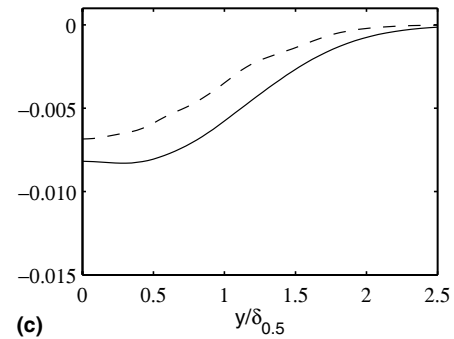
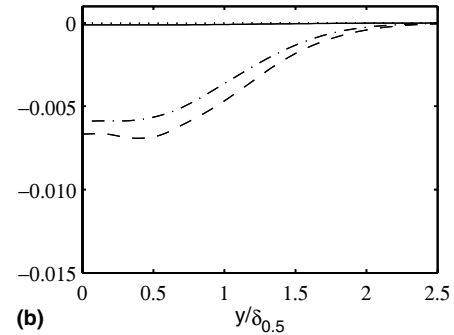
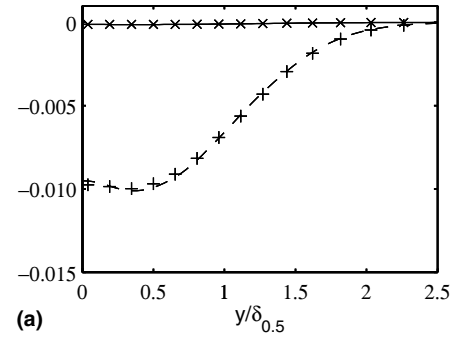


Fig. 7. Dissipation rates and DSM contributions to the energy budget across $x = 20r_0$. (a) LESsf: — molecular viscosity, - - - filtering, LESsf2: \times molecular viscosity, + filtering; (b) LESdsm2: — molecular viscosity, - - - filtering, - · - · eddy viscosity, $\cdots\cdots$ SGS energy and (c) LESre2: — molecular viscosity, - - - filtering.

To characterize the scales affected by the different dissipation mechanisms, the one-dimensional spectra of u' —velocity, $E_u^{(1)}(k_1)$ where k_1 is the axial wave number, have been calculated at $x = 20r_0$ on the jet axis. The features of the dissipations as a function of the wave number k_1 are then obtained by considering the following quantities: $\nu k_1^2 E_u^{(1)}(k_1)$ for the molecular viscosity, $\langle v_t \rangle k_1^2 E_u^{(1)}(k_1)$ for the eddy viscosity, and $D_{sf}(k_1 \Delta x) E_u^{(1)}(k_1)$ for the filtering, where D_{sf} is the transfer function of the filtering procedure used. The corresponding curves are presented in Fig. 8 for the simulations LESsf and LESsf2, LESdsm2 and LESre2.

Fig. 8(a) and (b) illustrate clearly that the selective filtering and the eddy viscosity dissipate energy through different turbulent scales: the filtering through the smaller resolved scales located beyond the filter cutoff wave number k_c^f , represented here by a vertical dotted line, and the eddy viscosity through a wide range of scales including

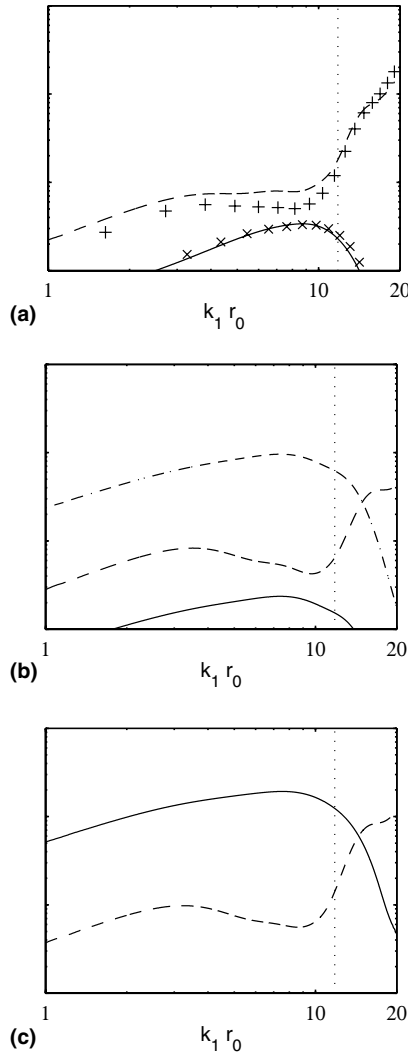


Fig. 8. Features of the different dissipation mechanisms for $x = 20r_0$ and $r = 0$, as a function of the axial wave number k_1 : (a) LESsf: — molecular viscosity, - - - filtering, LESsf2: \times molecular viscosity, + filtering; (b) LESdsm2 and (c) LESre2: — molecular viscosity, - - - filtering, - · - eddy-viscosity contribution. The curves are normalized by u_j^3 . The logarithmic Y-axis scale ranges from 4×10^{-8} up to 4×10^{-5} . The dotted line represents the filtering cutoff wave number $k_c^f = \pi/(2\Delta x)$ whereas the grid cutoff wave number is $k_c^g = \pi/\Delta x$.

the larger ones. This may be a major deficiency of eddy-viscosity models, especially at high Reynolds number where the dissipation on the large scales must be very small. The shape of the dissipation curve due to eddy viscosity in LESdsm2, in Fig. 8(b), is also very similar to that due to molecular viscosity in LESre2 at $Re_D = 5 \times 10^3$, in Fig. 8(c). Since eddy and molecular viscosities have the same functional form, they act similarly on the turbulent scales.

Finally in Fig. 8(a), there are only very little differences between LESsf, and LESsf2, where the filtering is applied at a lower strength. In both cases, energy is dissipated through the small scales such that $k_1 > k_c^f$, and the dissipation on the large scales such that $k_1 < k_c^f$ is very small. However, the amount of dissipation on the large scales

increases when the filtering is applied more frequently, and therefore would have to be checked for a frequency of application significantly higher than in the present simulations. Note also that in the high Reynolds number jet considered, the effects of the explicit filtering on the large scales are stronger than those of molecular viscosity. Ideally, this should be avoided. Unfortunately, at sufficiently high Reynolds numbers, the effects of molecular viscosity are negligible and it is difficult to meet this requirement because of the numerical dissipation, even when very low dissipation space and time discretization schemes are used.

5. Conclusions

In this work, Mach 0.9, round free jets at different Reynolds numbers have been simulated using low-dissipation schemes. In order to take into account the effects of the subgrid scales, a selective filtering was applied explicitly with and without dynamic Smagorinsky model. The flow developments have been compared. Kinetic energy budgets have also been calculated and the different dissipation mechanisms have been investigated. The main results are the following:

- In the LES using selective filtering alone, flow and dissipation features are shown to be independent of the filtering strength, because of the high selectivity of the filter. The filtering dissipates energy through the smaller resolved scales, and its contribution to the total energy dissipation is higher as the Reynolds number increases.
- The influence of the Reynolds number on the jet development appears to be well reproduced in the LES using the filtering alone. This point shows that the effective Reynolds number of the simulated jets agrees well with the Reynolds number $Re_D = u_j D/\nu$ given by the initial conditions using this LES approach.
- In the LES using DSM, a significant part of the energy is dissipated by the eddy viscosity through a wide range of turbulent scales including the larger ones. Since eddy viscosity has the same functional form as molecular viscosity, the effective flow Reynolds number is artificially decreased down to about $\tilde{Re}_D = u_j D/\nu_t$. This point is strongly supported by the flow development obtained from the LES using DSM which are similar to those observed at lower Reynolds numbers.
- The use of a subgrid-scale kinetic energy in DSM has no significant influence neither on the flow properties nor on the kinetic energy budget.

It is hoped that the present results would be of interest to point out the special features of the explicit selective filtering and of the subgrid-scale models based on eddy-viscosity. They show the crucial importance of the additional dissipations used in LES to take into account the effects of the subgrid scales. Eddy-viscosity models appear not to be recommended to study flow phenomena,

such as jet noise (Bogey and Bailly, 2006b), where the Reynolds number is a key parameter. In that case, the explicit filtering approach may be one of the appropriate ways.

Acknowledgements

This work was supported by the French network RRIT “Recherche Aéronautique sur le Supersonique” (Ministère de la Recherche). The simulations were performed on a Nec SX5 of the Institut du Développement et des Ressources en Informatique Scientifique (IDRIS–CNRS).

References

- Akhavan, R., Ansari, A., Kang, S., Mangiavacchi, N., 2000. Subgrid-scale interactions in a numerically simulated planar turbulent jet and implications for modelling. *J. Fluid Mech.* 408, 83–120.
- Andersson, N., Eriksson, L.-E., Davidson, L., 2005. Large-eddy simulation of subsonic turbulent jets and their radiated sound. *AIAA J.* 43 (9), 1899–1912.
- Arakeri, V.H., Krothapalli, A., Siddavaram, V., Alkislar, M.B., Lourenco, L., 2003. On the use of microjets to suppress turbulence in a Mach 0.9 axisymmetric jet. *J. Fluid Mech.* 490, 75–90.
- Bodony, D.J., Lele, S.K., 2005. On using large-eddy simulation for the prediction of noise from cold and heated turbulent jets. *Phys. Fluids* 17, 085130.
- Bogey, C., Bailly, C., 2004. A family of low dispersive and low dissipative explicit schemes for flow and noise computations. *J. Comput. Phys.* 194 (1), 194–214.
- Bogey, C., Bailly, C., 2005a. Effects of inflow conditions and forcing on subsonic jet flows and noise. *AIAA J.* 43 (5), 1000–1007.
- Bogey, C., Bailly, C., 2005b. Decrease of the effective Reynolds number with eddy-viscosity subgrid-scale modeling. *AIAA J.* 43 (2), 437–439.
- Bogey, C., Bailly, C., 2005c. Computation of the self-similarity region of a turbulent round jet using large eddy simulation. In: *Proceedings of Direct and Large-Eddy Simulation-6*, 12–14 September 2005, Poitiers, France.
- Bogey, C., Bailly, C., 2006a. Computation of a high Reynolds number jet and its radiated noise using LES based on explicit filtering. *Comput. Fluids*, to appear.
- Bogey, C., Bailly, C., 2006b. Investigation of downstream and sideline subsonic jet noise using large eddy simulation. *Theoret. Comput. Fluid Dynamics* 20 (1), 23–40.
- Da Silva, C.B., Métais, O., 2002. On the influence of coherent structures upon interscale interactions in turbulent plane jets. *J. Fluid Mech.* 473, 103–145.
- Domaradski, J.A., Yee, P.P., 2000. The subgrid-scale estimation model for high Reynolds number turbulence. *Phys. Fluids* 12 (1), 193–196.
- Erlebacher, G., Hussaini, M.Y., Speziale, C.G., Zang, T.A., 1992. Toward the large-eddy simulation of compressible turbulent flows. *J. Fluid Mech.* 238, 155–185.
- Freund, J.B., 2001. Noise sources in a low-Reynolds-number turbulent jet at Mach 0.9. *J. Fluid Mech.* 438, 277–305.
- Le Ribault, C., Sarkar, S., Stanley, S.A., 1999. Large eddy simulation of a plane jet. *Phys. Fluids* 11 (10), 3069–3083.
- Lilly, D.K., 1992. A proposed modification of the Germano subgrid-scale closure method. *Phys. Fluids* A 4 (3), 633–635.
- Mathew, J., Lechner, R., Foysi, H., Sesterhenn, J., Friedrich, R., 2003. An explicit filtering method for large eddy simulation of compressible flows. *Phys. Fluids* 15 (8), 2279–2289.
- Michalke, A., 1984. Survey on jet instability theory. *Prog. Aerospace Sci.* 21, 159–199.
- Moin, P., Squires, K., Cabot, W., Lee, S., 1991. A dynamic subgrid-scale model for compressible turbulence and scalar transport. *Phys. Fluids* 3 (11), 2746–2757.
- Panchapakesan, N.R., Lumley, J.L., 1993. Turbulence measurements in axisymmetric jets of air and helium. Part I. Air jet. *J. Fluid Mech.* 246, 197–223.
- Rizzetta, D.P., Visbal, M.R., Blaisdell, G.A., 2003. A time-implicit high-order compact differencing and filtering scheme for large-eddy simulation. *Int. J. Numer. Meth. Fluids* 42 (6), 665–693.
- Speziale, C.G., Erlebacher, G., Zang, T.A., Hussaini, M.Y., 1988. The subgrid-scale modeling of compressible turbulence. *Phys. Fluids* 31 (4), 940–942.
- Stolz, S., Adams, N.A., Kleiser, L., 2001. An approximate deconvolution model for large-eddy simulation with application to incompressible wall-bounded flows. *Phys. Fluids* 13 (4), 997–1015.
- Stromberg, J.L., McLaughlin, D.K., Troutt, T.R., 1980. Flow field and acoustic properties of a Mach number 0.9 jet at a low Reynolds number. *J. Sound Vib.* 72 (2), 159–176.
- Visbal, M.R., Rizzetta, D.P., 2002. Large-eddy simulation on curvilinear grids using compact differencing and filtering schemes. *J. Fluids Eng.* 124, 836–847.
- Vreman, B., Geurts, B., Kuerten, H., 1997. Large-eddy simulation of the turbulent mixing layer. *J. Fluid Mech.* 339, 357–390.
- Wynanski, I., Fiedler, H., 1969. Some measurements in the self-preserving jet. *J. Fluid Mech.* 38 (3), 577–612.